Cell Reports, Volume *26*

Supplemental Information

Blockade of MCU-Mediated Ca^{2+} Uptake Perturbs Lipid Metabolism via PP4-Dependent AMPK Dephosphorylation

Dhanendra Tomar, Fabián Jaña, Zhiwei Dong, William J. Quinn III, Pooja Jadiya, Sarah L. Breves, Cassidy C. Daw, Subramanya Srikantan, Santhanam Shanmughapriya, Neeharika Nemani, Edmund Carvalho, Aparna Tripathi, Alison M. Worth, Xueqian Zhang, Roshanak Razmpour, Ajay Seelam, Stephen Rhode, Anuj V. Mehta, Michael Murray, Daniel Slade, Servio H. Ramirez, Prashant Mishra, Glenn S. Gerhard, Jeffrey Caplan, Luke Norton, Kumar Sharma, Sudarsan Rajan, Darius Balciunas, Dayanjan S. Wijesinghe, Rexford S. Ahima, Joseph A. Baur, and Muniswamy Madesh

SUPPLEMENTAL INFORMATION

Blockade of MCU-Mediated Ca^{2+} Uptake Perturbs Lipid Metabolism via PP4-Dependent AMPK Dephosphorylation

Dhanendra Tomar,[1,2] Fabián Jaña,[1,2] Zhiwei Dong,[1,2] William J. Quinn III,[3] Pooja Jadiya,[2] Sarah L Breves,[1,2] Cassidy C Daw[10], Subbramanya Srikantan[10], Santhanam Shanmughapriya,[1,2] Neeharika Nemani,[1,2] Edmund Carvalho,[1,2], Aparna Tripathi,[1,2] Alison M. Worth,[1,2] Xueqian Zhang,[2] Roshanak Razmpour,[4] Ajay Seelam,[1,2] Stephen Rhode,[1,2] Anuj V Mehta,[2,5] Michael Murray,[1,2] Daniel Slade,[1,2] Servio H. Ramirez,[4] Prashant Mishra,[6] Glenn S Gerhard,[1] Jeffrey Caplan,[7] Luke Norton[11], Kumar Sharma[10], Sudarsan Rajan,[1,2] Darius Balciunas,[5] Dayanjan S. Wijesinghe[8], Rexford S. Ahima[9], Joseph A. Baur,[3] and Muniswamy Madesh[1,2,10*]

A
MCU^fl/fl
MCU^Δhep
Normalized mRNA Expression
1.5
1.0
0.5
0.0
***
ns
MCU
MCUR1

B
Rhod123
TMRM
Merge
MCU^fl/fl
MCU^Δhep
20μm

H
MCU^fl/fl
MCU^Δhep
MCU
MCUR1
MICU1
OXPHOS
CV
CIII
CIV
CII
CI
ATP5A
TOM20

C
TMRM (arb unit)
1500
1000
500
0
ns
MCU^fl/fl
MCU^Δhep

D
Rhod123
MitoSOX
Merge
MCU^fl/fl
MCU^Δhep
20μm

E
MitoSOX (arb unit)
120
100
80
60
40
20
0
***
MCU^fl/fl
MCU^Δhep

F
Glucose
OCR (pmol/min/μg protein)
80
60
40
20
0
Oligo
FCCP
A+R
MCU^fl/fl
MCU^Δhep
0
20
40
60
80
Time (min)

G
MCU^fl/fl
MCU^Δhep
OCR (pmol/min/μg protein)
70
60
50
40
30
20
10
0
***
**
***
Basal
ATP Coupled
Maximal

I
MCU^fl/fl
MCU^-/-
1 2 3 1 2 3
CPT1
MCU
TOM20

J
CPT1/TOM20 Ratio
0.8
0.6
0.4
0.2
0.0
ns
MCU^fl/fl
MCU^Δhep

K
MCU^fl/fl
MCU^-/-
1 2 1 2
PGC1α
mtTFA
NRF1
MCU
βActin
TOM20

L
MCU^fl/fl
MCU^Δhep
Protein/TOM20 Ratio
0.8
0.6
0.4
0.2
0.0
ns
ns
ns
PGC1α
mtTFA
NRF1

Figure S1 (Related to Figure 1): Assessment of hepatocyte-specific MCU knockout mice, mitochondrial membrane potential, oxygen consumption rate, and mitochondrial biogenesis-related proteins abundance

(A) MCU and MCUR1 mRNA abundance were quantitated in hepatocytes isolated from $MCU^{fl/fl}$ and $MCU^{\Delta hep}$ mice. Mean ± SEM; ***p < 0.001; ns= not significant; n = 4 mice. **(B)** MCU deletion in hepatocytes does not affect $\Delta\Psi_m$. Representative confocal images of primary hepatocytes from $MCU^{fl/fl}$ and $MCU^{\Delta hep}$ mice loaded with $\Delta\Psi_m$ indicator, TMRM (50nM). Scale bar= 20μm. n = 3 mice. **(C)** Quantification of TMRM fluorescence as an indicator of $\Delta\Psi_m$. Mean ± SEM; ns= not significant; n = 3 mice. **(D)** Elimination of MCU results in reduced mitochondrial ROS generation. Representative confocal images of primary hepatocytes from $MCU^{fl/fl}$ and $MCU^{\Delta hep}$ mice loaded with mitochondrial superoxide indicator, MitoSOX™ Red (2 μM). Scale bar= 20μm. n = 3 mice. **(E)** Quantification of MitoSOX™ Red fluorescence from raw images of Figure S1D, as an indicator of mitochondrial superoxide generation. Mean ± SEM; ***p < 0.001; n = 3 mice. **(F)** The mitochondrial Oxygen consumption rate (OCR). OCR was measured in $MCU^{fl/fl}$ and $MCU^{\Delta hep}$ hepatocytes using the Seahorse XF Analyzer. Mean ± SEM. n = 3 mice. **(G)** After basal OCR was recording, oligomycin, FCCP, and antimycin A + rotenone were added and ATP coupled and maximal OCR were calculated from Figure S1F. Mean ± SEM. **p < 0.01, and ***p < 0.001. n = 3 mice. **(H)** MCU-KO does not affect the expression of respiratory chain complex proteins. Western blot analysis of MCU-complex (MCU, MCUR1, MICU1) and mitochondrial respiratory chain subunits complex I (NDUFB8), complex II (SDHB), complex III (UQCRC2), complex IV (MTCO1) and ATP synthase subunit ATP5A in $MCU^{fl/fl}$ and $MCU^{\Delta hep}$ hepatocytes. TOM20 was used as a loading control. n = 3 mice. **(I)** CPT1 protein expression in $MCU^{\Delta hep}$ hepatocytes. Hepatocytes isolated from $MCU^{fl/fl}$ and $MCU^{\Delta hep}$ mice were lysed in RIPA buffer and probed with indicated antibodies. n= 3 mice. **(J)** Bar graph represents densitometric analysis of CPT1 protein abundance. Data represented as mean ± SEM. ns= non-significant p value. n= 3 mice. **(K)** MCU-KO does not have any effect on mitochondrial biogenesis-regulating transcription factors. Hepatocytes isolated from 10-12 week old $MCU^{fl/fl}$ and $MCU^{\Delta hep}$ mice were lysed in RIPA buffer and probed with indicated antibodies. n= 4. **(L)** Bar graph represents densitometric analysis of mitochondrial biogenesis-regulating transcription factors protein abundance. Mean ± SEM. ns= non-significant. n= 4.

S2

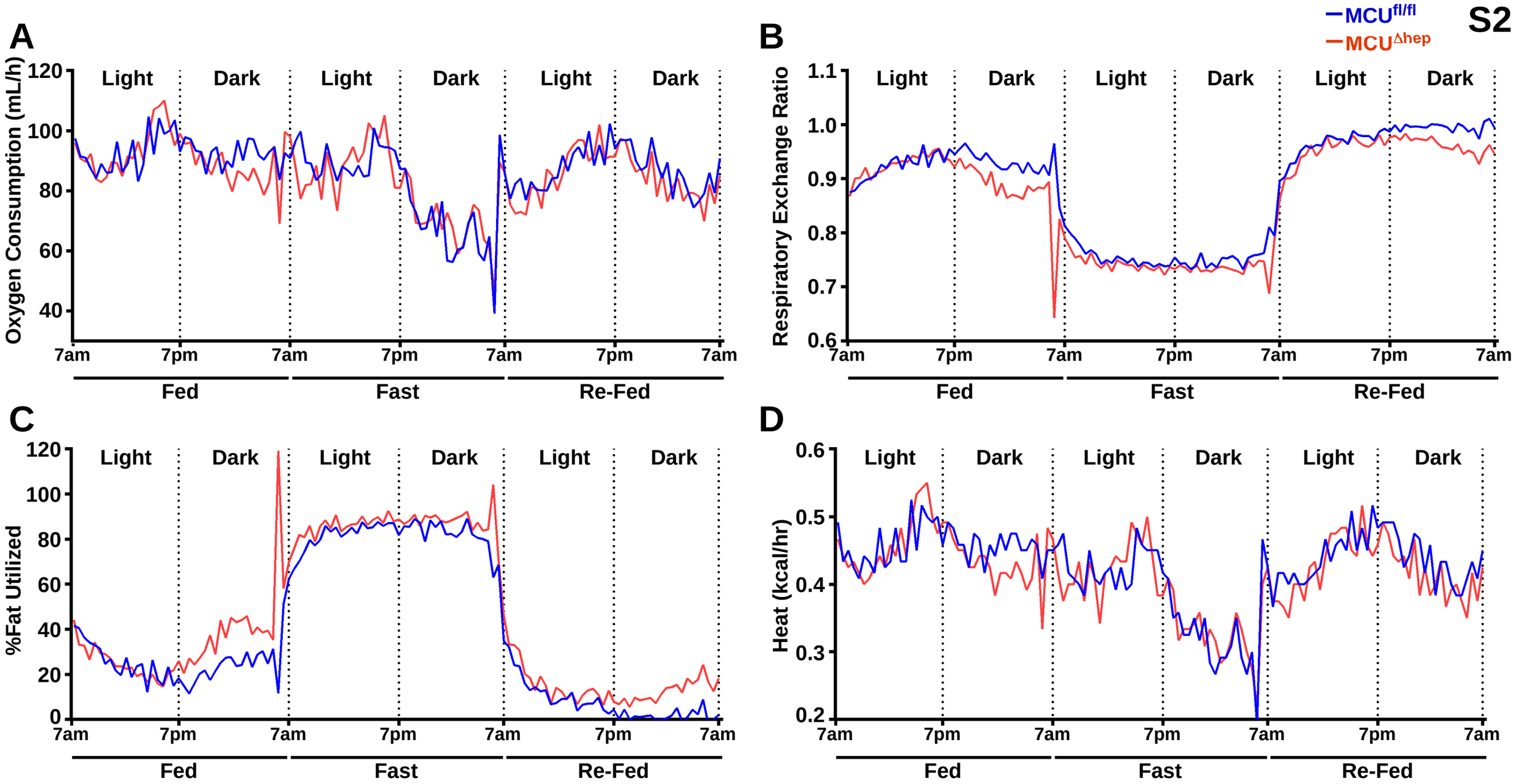
MCU^fl/fl
MCU^Δhep
A
Oxygen Consumption (mL/h)
120
100
80
60
40
Light
Dark
Light
Dark
Light
Dark
7am
7pm
7am
7pm
7am
7pm
7am
Fed
Fast
Re-Fed
B
Respiratory Exchange Ratio
1.1
1.0
0.9
0.8
0.7
0.6
C
%Fat Utilized
D
Heat (kcal/hr)
0.6
0.5
0.4
0.3
0.2
E
Locomotor Activity (a.u.)
4000
3000
2000
1000
0
F
Food Intake (g/h)
0.4
0.3
0.2
0.1
0.0

Figure S2 (Related to Figure 1): Assessment of the metabolic profiles of the mice.

(A-F) $MCU^{fl/fl}$ and $MCU^{\Delta hep}$ mice 8-10 weeks old were fed a normal chow diet and studied in a Comprehensive Animal Monitoring System (CLAMS, Columbus Instruments, Columbus, OH). **(A)** Oxygen consumption, **(B)** respiratory exchange ratio, **(C)** %Fat utilized, **(D)** Heat generated, **(E)** locomotor activity, and **(F)** food intake were measured (n = 10-12 mice per group).

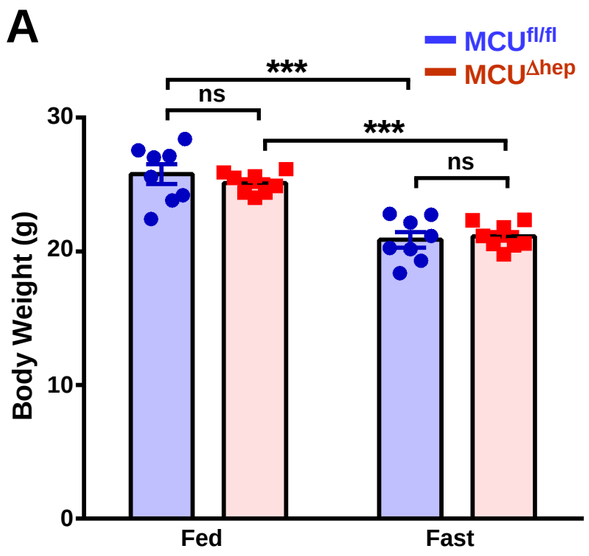
A
MCUfl/fl
MCUΔhep
***
ns
***
ns
Body Weight (g)
30
20
10
0
Fed
Fast

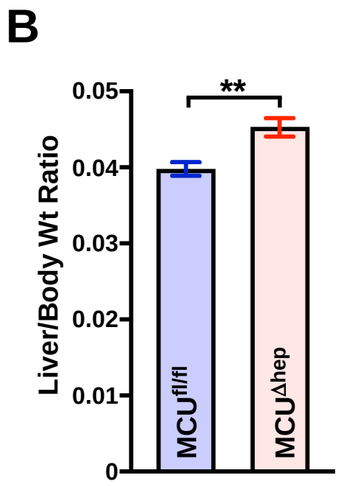
B
**
Liver/Body Wt Ratio
0.05
0.04
0.03
0.02
0.01
0
MCUfl/fl
MCUΔhep

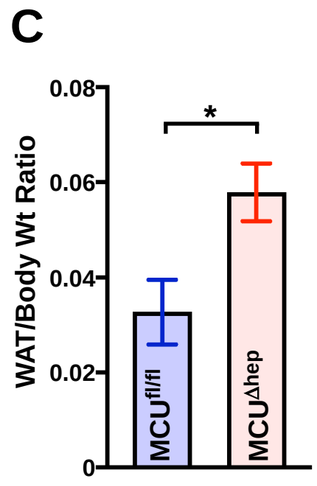
C
*
WAT/Body Wt Ratio
0.08
0.06
0.04
0.02
0
MCUfl/fl
MCUΔhep

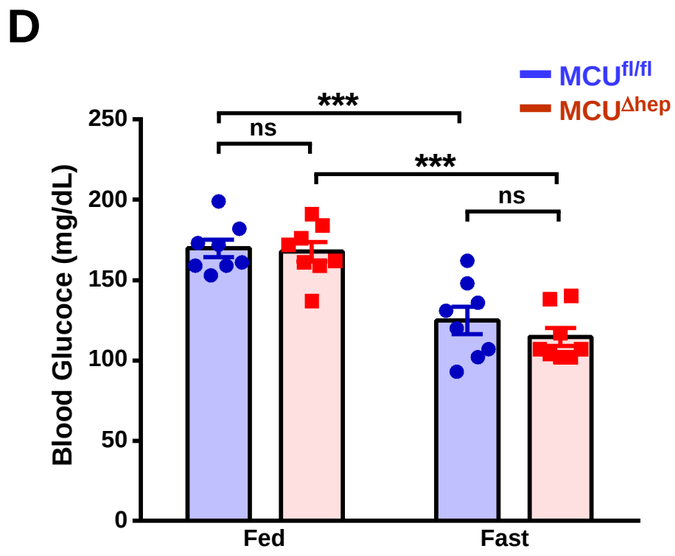
D
MCUfl/fl
MCUΔhep
***
ns
***
ns
Blood Glucose (mg/dL)
250
200
150
100
50
0
Fed
Fast

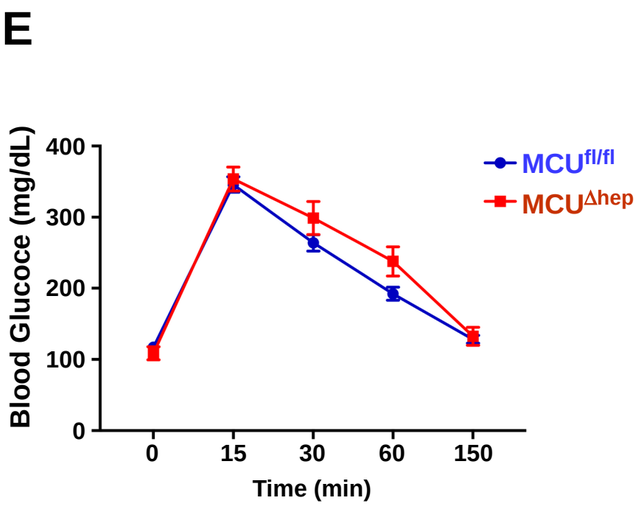
E
Blood Glucose (mg/dL)
400
300
200
100
0
MCUfl/fl
MCUΔhep
0
15
30
60
150
Time (min)

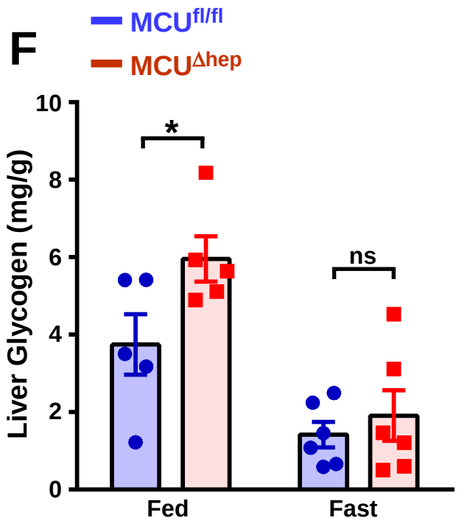
F
MCUfl/fl
MCUΔhep
Liver Glycogen (mg/g)
10
8
6
4
2
0
*
ns
Fed
Fast

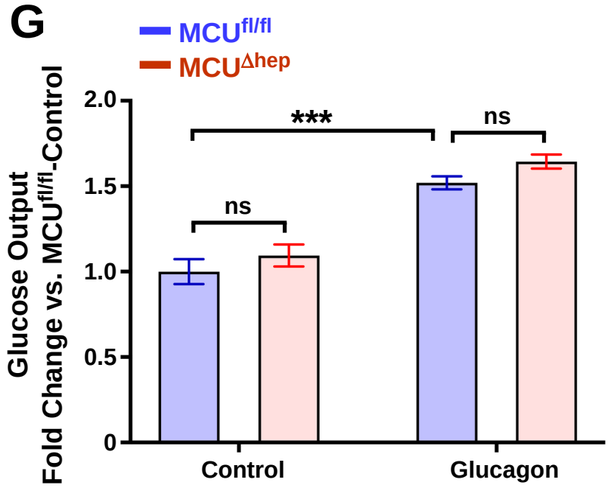
G
MCUfl/fl
MCUΔhep
Glucose Output
Fold Change vs. MCUfl/fl-Control
2.0
1.5
1.0
0.5
0
***
ns
ns
Control
Glucagon

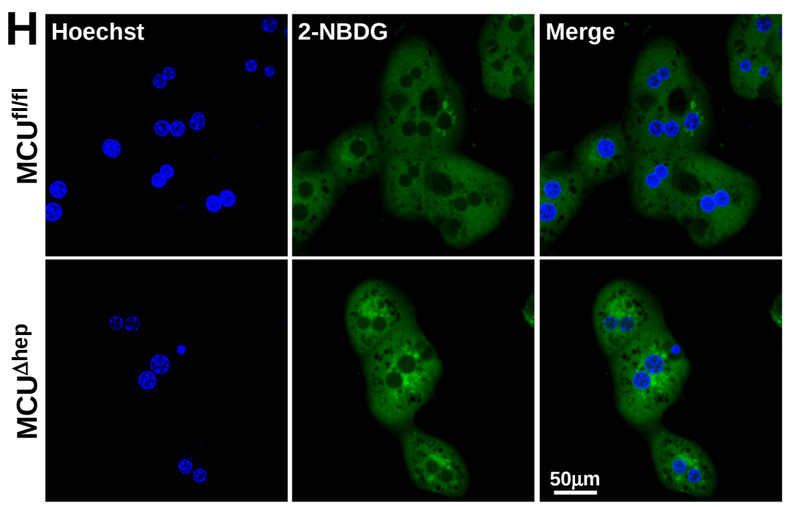
H
Hoechst
2-NBDG
Merge
MCUfl/fl
MCUΔhep
50μm

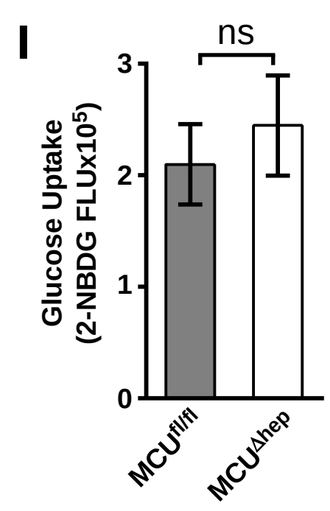
I
ns
Glucose Uptake
(2-NBDG FLUx10^5)
3
2
1
0
MCUfl/fl
MCUΔhep

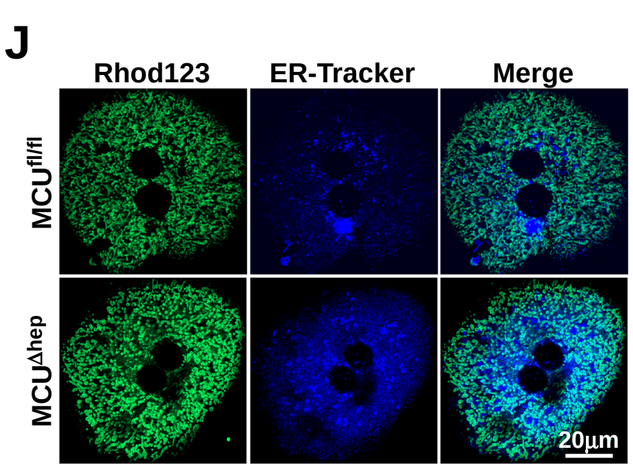
J
Rhod123
ER-Tracker
Merge
MCUfl/fl
MCUΔhep
20μm

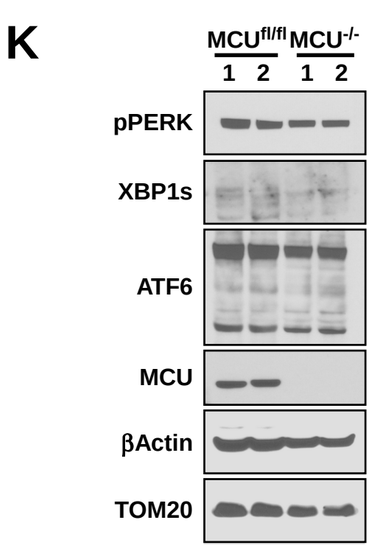
K
MCUfl/fl
MCU-/-
1 2 1 2
pPERK
XBP1s
ATF6
MCU
βActin
TOM20

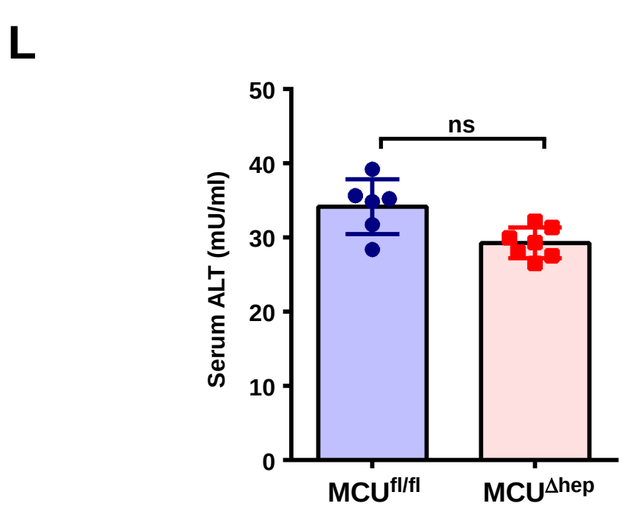
L
Serum ALT (mU/ml)
50
40
30
20
10
0
ns
MCUfl/fl
MCUΔhep

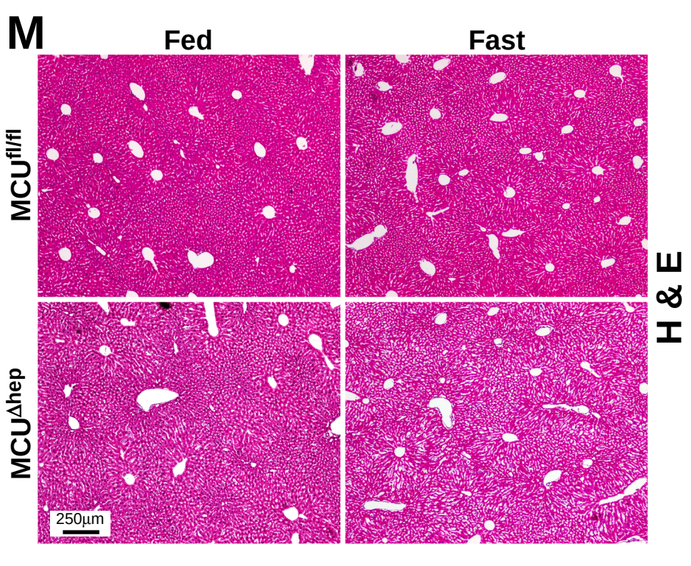
M
Fed
Fast
MCUfl/fl
MCUΔhep
H & E
250μm

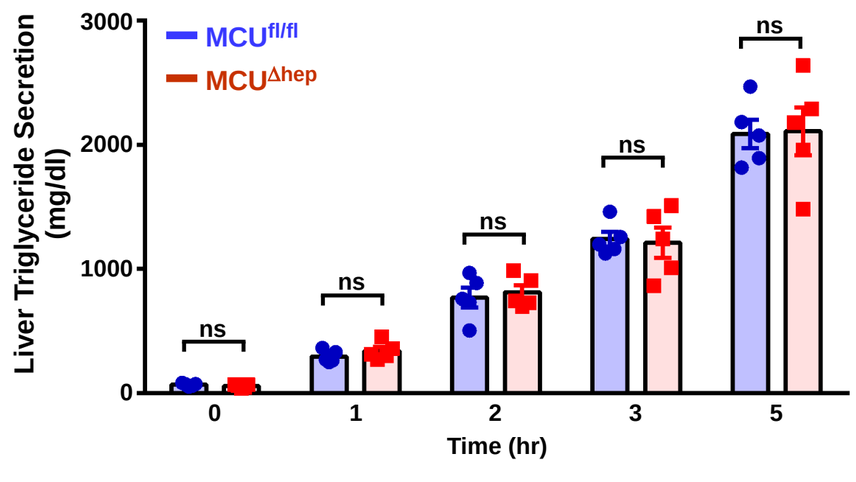
N
Liver Triglyceride Secretion
(mg/dl)
3000
2000
1000
0
MCUfl/fl
MCUΔhep
ns
0
1
2
3
5
Time (hr)

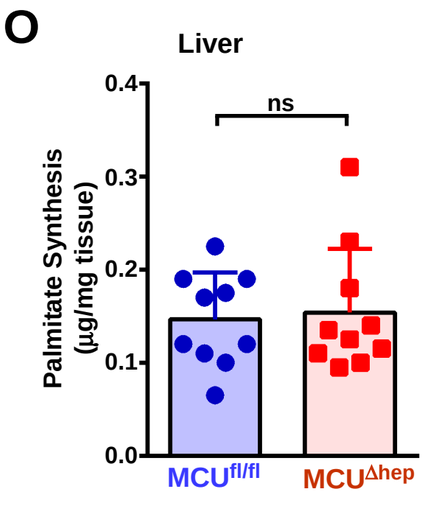
O
Liver
Palmitate Synthesis
(μg/mg tissue)
0.4
0.3
0.2
0.1
0.0
ns
MCUfl/fl
MCUΔhep

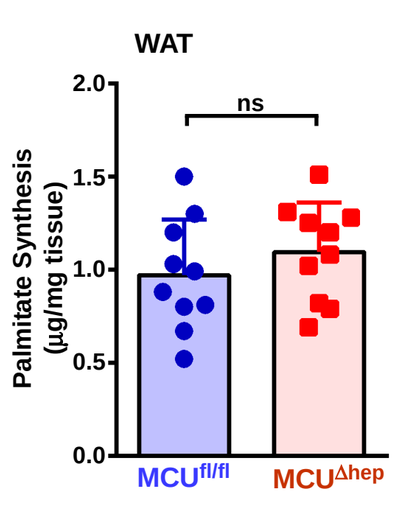
P
WAT
Palmitate Synthesis
(μg/mg tissue)
2.0
1.5
1.0
0.5
0.0
ns
MCUfl/fl
MCUΔhep

Figure S3 (Related to Figure 2): Body weight, glucose/glycogen measurements, liver injury assay, liver H&E staining, ER distribution and ER stress, liver TAG secretion, and de novo lipogenesis.

(A) Loss of MCU in hepatic tissue does not alter the gross body weight. Nuclear Magnetic Resonance (NMR) and Dual-Energy X-ray absorptiometry (DEXA) are used for the assessment of 8-week-old $MCU^{fl/fl}$ and $MCU^{\Delta hep}$ mice body composition. Mice were fed a normal chow diet and fasted for 24 hours. Body mass was monitored using NMR before and after fasting. Mean ± SEM. ***p < 0.001, ns= non-significant p value; n = 8 mice per group. **(B and C)** $MCU^{\Delta hep}$ mice demonstrate significantly increased liver/body wt and WAT/body wt ratio as compared to the $MCU^{fl/fl}$ mice. The body weight of 8-week old mice was measured, and then liver lobes and WAT was excised for quantification of tissue weights, plotted as tissue/total body wt ratio. Mean ± SEM. **p < 0.01, and *p < 0.05. n = 5-11 mice. **(D)** Blood glucose levels were unchanged in $MCU^{\Delta hep}$ mice. Tail blood was drawn from 8-week-old $MCU^{fl/fl}$ and $MCU^{\Delta hep}$ mice that were fed a normal chow diet and allowed to fast for 24 hours. Blood glucose was measured by an OneTouch Ultra glucometer. Mean ± SEM. ***p < 0.001, ns= non-significant p value; n = 8 mice per group. **(E)** Loss of *Mcu* does not alter glucose tolerance in mice. The glucose tolerance test was performed as described in the methods section. n = 10 mice per group. **(F)** Hepatic deletion of MCU leads to increased glycogen content in the liver during fed state. Liver tissue collected from fed and 24 hours fasted mice were used for the estimation of liver glycogen using enzymatic assay. Mean ± SEM. *p < 0.05, ns= non-significant p value; n = 5-6 mice per group. **(G)** Loss of *Mcu* does not alter hepatocyte glucose output. The glucose output assay was performed on primary hepatocytes in response to glucagon, and plotted as fold change compared to the $MCU^{fl/fl}$ hepatocytes. Mean ± SEM; ***p < 0.001, ns= not significant. **(H)** MCU-KO in hepatocytes does not affect hepatic glucose uptake. Glucose uptake was visualized by confocal microscope after culturing the hepatocytes from $MCU^{fl/fl}$ and $MCU^{\Delta hep}$ mice with 2-NBDG instead of glucose. Hoechst stain was used to visualize nuclei. n= 3 mice. **(I)** Bar graph for the quantification of 2-NBDG fluorescence as an indicator of glucose uptake. Mean ± SEM; ns= not significant. n= 3 mice. **(J)** MCU-KO does not affect endoplasmic reticulum distribution. Hepatocytes isolated from $MCU^{fl/fl}$ and $MCU^{\Delta hep}$ mice were stained with Rhod123 and ER-tracker Blue. Distribution of mitochondria and ER was visualized by confocal imaging. n= 3. **(K)** Loss of MCU in hepatocytes does not show altered ER-stress. Hepatocytes isolated from 10-12 week old $MCU^{fl/fl}$ and $MCU^{\Delta hep}$ mice were lysed in RIPA buffer and probed with indicated antibodies. n= 4 mice. **(L)** Bar graph showing plasma ALTase activity as a measure of liver injury. Mean ± SEM; ns= not

significant; n = 3 mice. **(M)** MCU-KO liver section does not show any gross morphological alterations. Liver from $MCU^{fl/fl}$ and $MCU^{\Delta hep}$ mice were perfused, fixed, and stained with H&E. Representative histological section image (4 x magnification). n = 3 mice per group. **(N)** Loss of MCU in hepatic tissue does not alter the liver triglyceride secretion. **(O)** $MCU^{\Delta hep}$ mice have normal hepatic de novo lipogenesis as measured by palmitate synthesis. Mean ± SEM. ns= non-significant p value; n = 10 mice per group. **(P)** $MCU^{\Delta hep}$ mice have normal white adipose tissue (WAT) de novo lipogenesis as measured by palmitate synthesis. Mean ± SEM. ns= non-significant p value; n = 10 mice per group.

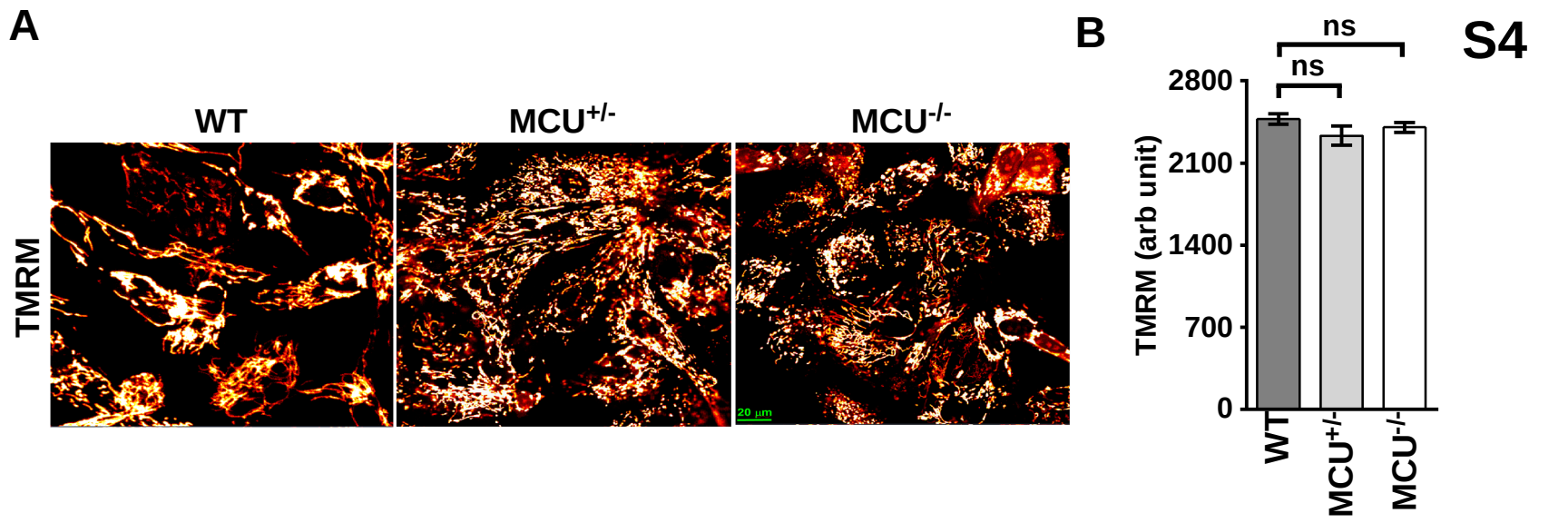
A
WT
MCU+/-
MCU-/-
TMRM
20 µm
B
S4
ns
ns
TMRM (arb unit)
2800
2100
1400
700
0
WT
MCU+/-
MCU-/-

Figure S4 (Related to Figure 3): Assessment of mitochondrial membrane potential ($\Delta\Psi_m$) in zebrafish primary cells.

(A) MCU deletion did not alter $\Delta\Psi_m$. Representative confocal images of primary cells from WT, $MCU^{+/-}$ and $MCU^{-/-}$ zebrafish stained with $\Delta\Psi_m$ indicator, TMRM (50nM). n = 3. **(B)** Quantification of TMRM fluorescence. Mean ± SEM; ns= not significant; n = 3.

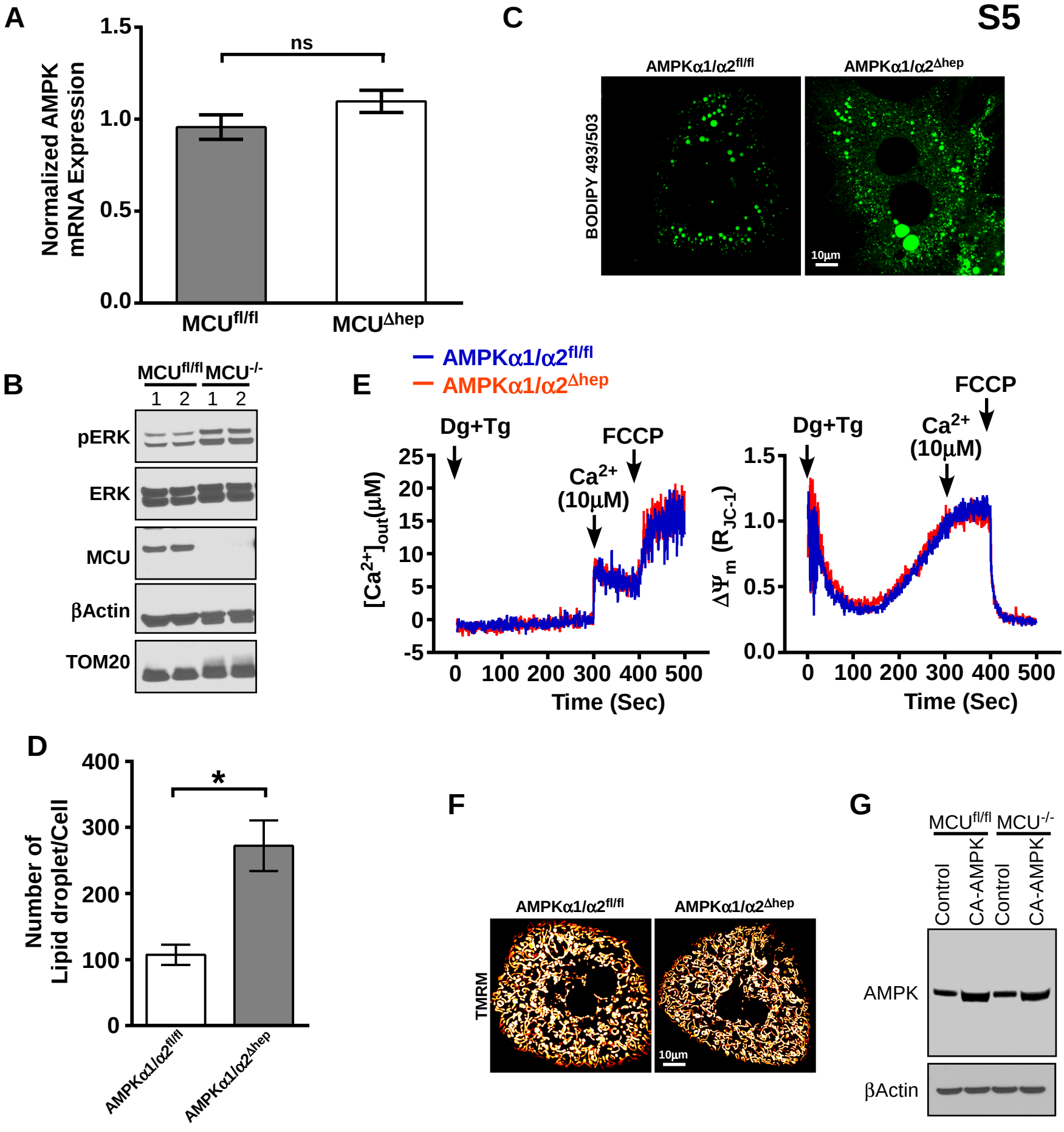
A
Normalized AMPK mRNA Expression
1.5
1.0
0.5
0.0
ns
MCU^fl/fl
MCU^Δhep
B
MCU^fl/fl MCU^-/-
1 2 1 2
pERK
ERK
MCU
βActin
TOM20
C
AMPKα1/α2^fl/fl
AMPKα1/α2^Δhep
BODIPY 493/503
10μm
D
Number of Lipid droplet/Cell
400
300
200
100
0
*
AMPKα1/α2^fl/fl
AMPKα1/α2^Δhep
E
AMPKα1/α2^fl/fl
AMPKα1/α2^Δhep
Dg+Tg
FCCP
Ca2+ (10μM)
[Ca2+]out(μM)
ΔΨm (RJC-1)
Time (Sec)
F
AMPKα1/α2^fl/fl
AMPKα1/α2^Δhep
TMRM
10μm
G
MCU^fl/fl
MCU^-/-
Control
CA-AMPK
Control
CA-AMPK
AMPK
βActin

Figure S5 (Related to Figure 4): AMPK mRNA abundance in $MCU^{\Delta hep}$ hepatocytes, ERK-phosphorylation in $MCU^{\Delta hep}$ hepatocytes, BODIPY493/503 staining, Ca^{2+} and $\Delta\Psi_m$ measurement in AMPK $\alpha1/\alpha2^{\Delta hep}$ hepatocytes, and reconstitution of CA-AMPK.

(A) AMPK mRNA abundance was quantified in hepatocytes isolated from $MCU^{fl/fl}$ and $MCU^{\Delta hep}$ mice. Mean ± SEM; ns= non- significant p value; n = 4 mice. **(B)** ERK phosphorylation is not suppressed in MCU-KO hepatocytes. Hepatocytes cell lysate prepared from $MCU^{fl/fl}$, $MCU^{\Delta hep}$, and probed with indicated antibodies. n= 4 mice. **(C)** Loss of AMPK$\alpha1/\alpha2$ results in the increased lipid droplets in primary hepatocytes. Lipid droplets were visualized by confocal microscopy after BODIPY® 493/503 staining in primary hepatocytes isolated from indicated genotype. n = 3. **(D)** Number of lipid droplets were quantified after BODIPY® 493/503 staining. Mean ± SEM. *$p < 0.05$; n=20-30 cells. **(E)** Loss of AMPK$\alpha1/\alpha2$ does not alter $_mCa^{2+}$ uptake and mitochondrial membrane potential. Representative traces of $[Ca^{2+}]_{out}$ clearance and $\Delta\Psi_m$ in hepatocytes from indicated genotypes. n = 3. **(F)** Hepatic deletion of AMPK$\alpha1/\alpha2$ does not affect $\Delta\Psi_m$. Representative confocal images of primary hepatocytes isolated from AMPK$\alpha1/\alpha2^{fl/fl}$ and AMPK$\alpha1/\alpha2^{\Delta hep}$ mice stained with $\Delta\Psi_m$ indicator, TMRM (50nM). n = 3 mice. **(G)** Primary hepatocytes isolated from $MCU^{fl/fl}$ and $MCU^{\Delta hep}$ mice were infected with control vector and CA-AMPK expressing adeno-virus. Cell lysate prepared and probed with AMPK antibody.

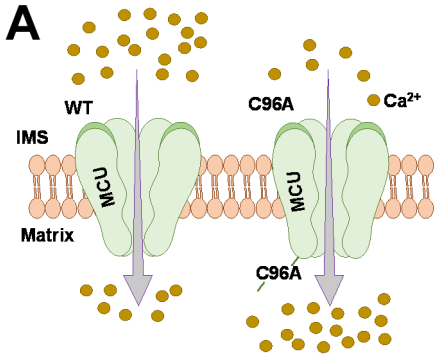
A
WT
C96A
Ca2+
IMS
MCU
MCU
Matrix
C96A

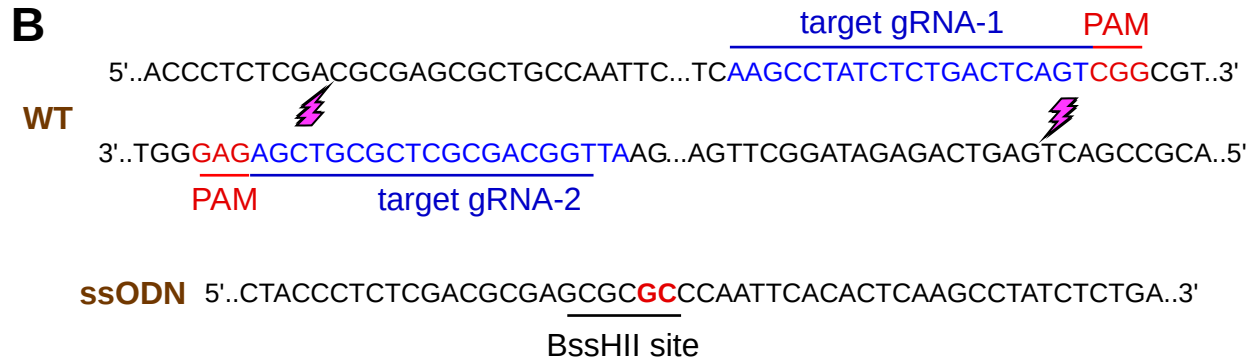
B
target gRNA-1
PAM
5'..ACCCTCTCGACGCGAGCGCTGCCAATTC...TCAAGCCTATCTCTGACTCAGTCGGCGT..3'
WT
3'..TGGGAGAGCTGCGCTCGCGACGGTTAAG...AGTTCGGATAGAGACTGAGTCAGCCGCA..5'
PAM
target gRNA-2
ssODN 5'..CTACCCTCTCGACGCGAGCGCGCCCAATTCACACTCAAGCCTATCTCTGA..3'
BssHII site

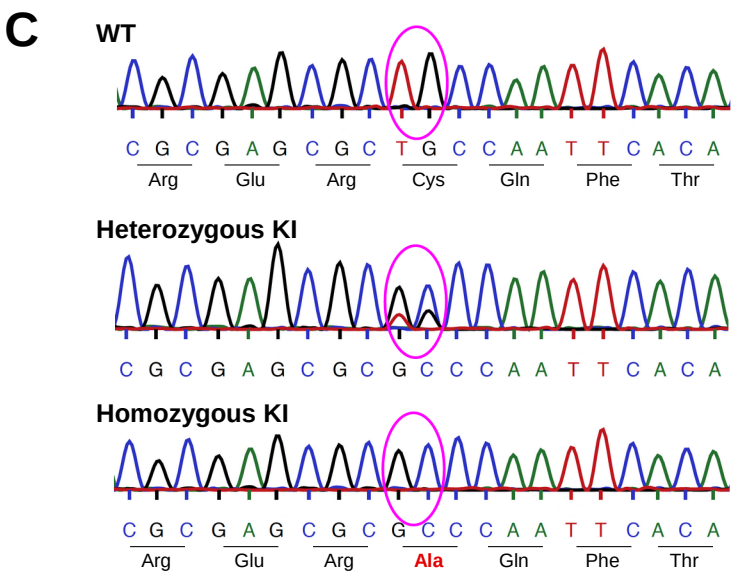
C
WT
C G C G A G C G C T G C C A A T T C A C A
Arg Glu Arg Cys Gln Phe Thr
Heterozygous KI
C G C G A G C G C G C C C A A T T C A C A
Homozygous KI
C G C G A G C G C G C C C A A T T C A C A
Arg Glu Arg Ala Gln Phe Thr

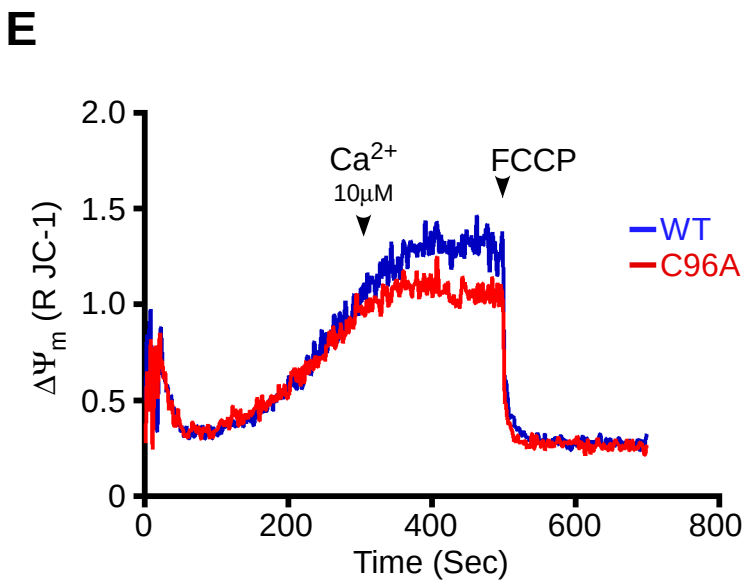
E
2.0
1.5
1.0
0.5
0
ΔΨm (R JC-1)
Ca2+
10μM
FCCP
WT
C96A
0
200
400
600
800
Time (Sec)

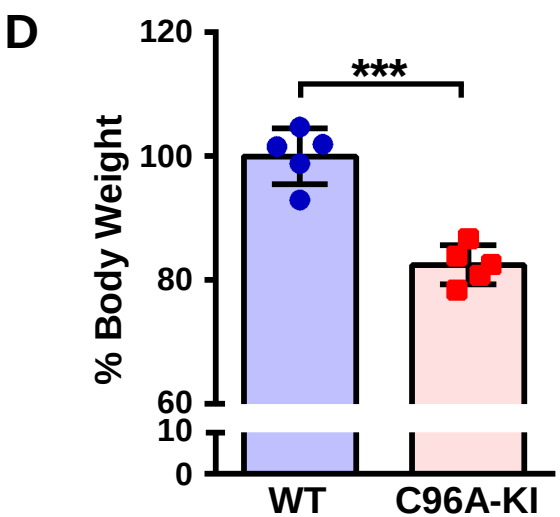
D
120
100
80
60
10
0
% Body Weight
***
WT
C96A-KI

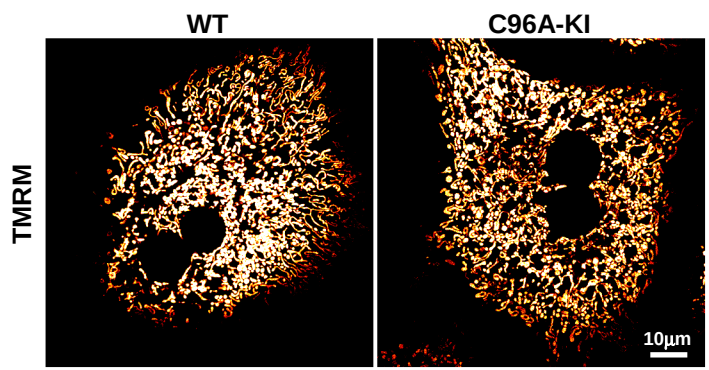
F
WT
C96A-KI
TMRM
10μm

Figure S6 (Related to Figure 6): Generation and validation of MCU-C96A KI mice and assessment of $\Delta\Psi_m$.

(A) Schematic represents the constitutive activation of MCU channel due to C96A mutation. **(B)** CRISPR/Cas9 (Nickase) mediated targeting of MCU- genomic region. **(C)** Sequencing data from the WT, heterozygous C96A-KI and homozygous C96A-KI animal shows the replacement of TGC (encode Cys) to GCC (encode Ala). **(D)** The relative body weight of WT and C96A-KI mice. Mean ± SEM. ***$p < 0.001$, $n = 5$. **(E)** MCU C96A KI does not affect the $\Delta\Psi_m$. WT and C96A-KI mice hepatocytes were isolated, permeabilized with digitonin (40 μg/mL) in intracellular like media containing thapsigargin (2 μM). The $\Delta\Psi_m$ indicator JC-1 was added at 20 seconds and after reaching steady state $\Delta\Psi m$. A bolus of extramitochondrial Ca^{2+} (10 μM) was added at the indicated time point before adding the mitochondrial uncoupler FCCP (2 μM). Representative traces of JC-1 staining showing the $\Delta\Psi m$ in permeabilized hepatocytes from WT and C96A-KI. $n = 3$. **(F)** C96A-KI does not affect $\Delta\Psi_m$. Representative confocal images of primary hepatocytes from WT and C96A-KI mice loaded with $\Delta\Psi_m$ indicator, TMRM (50nM). $n = 3$.

A

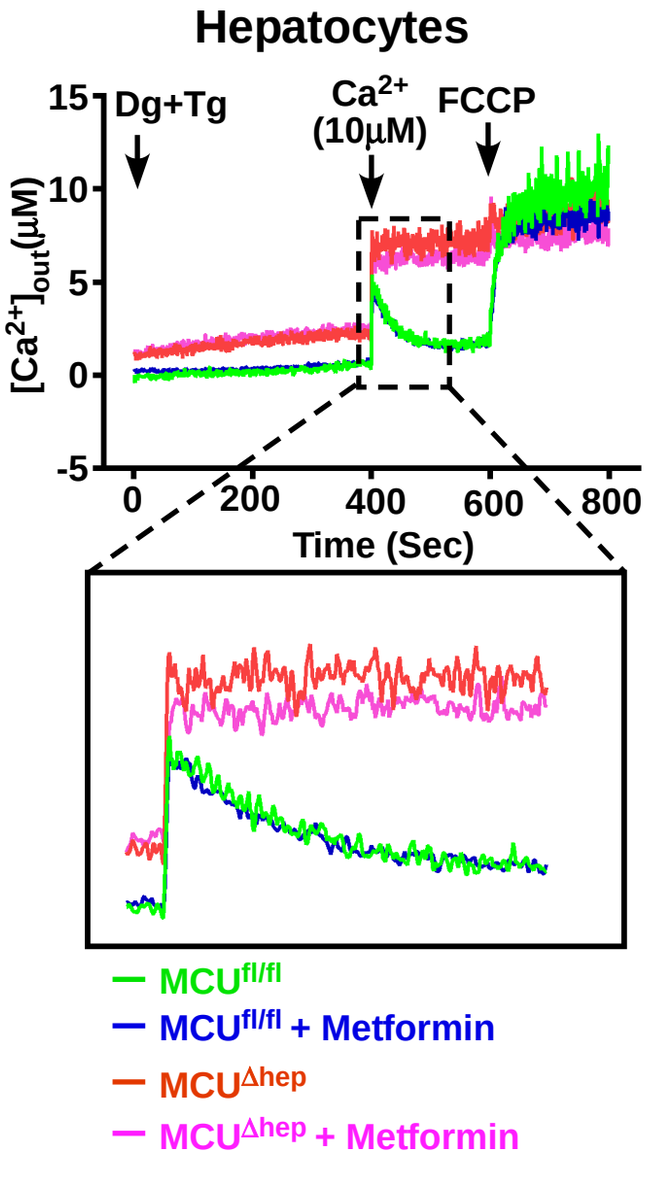
Hepatocytes
Dg+Tg
Ca2+ (10μM)
FCCP
[Ca2+]out(μM)
15
10
5
0
-5
0
200
400
600
800
Time (Sec)
MCUfl/fl
MCUfl/fl + Metformin
MCUΔhep
MCUΔhep + Metformin

B

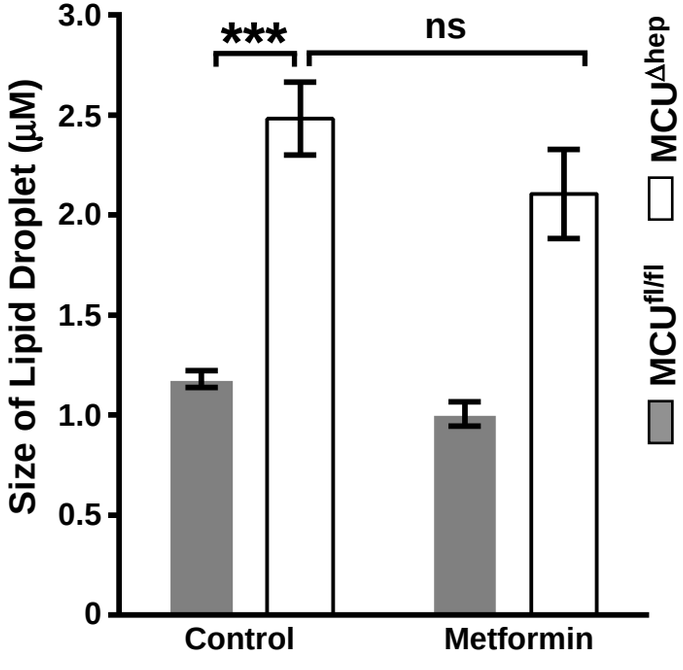
***
ns
Size of Lipid Droplet (μM)
3.0
2.5
2.0
1.5
1.0
0.5
0
Control
Metformin
MCUΔhep
MCUfl/fl

C

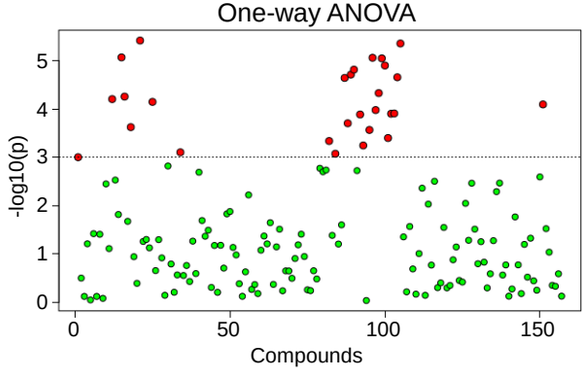
One-way ANOVA
-log10(p)
5
4
3
2
1
0
0
50
100
150
Compounds

D

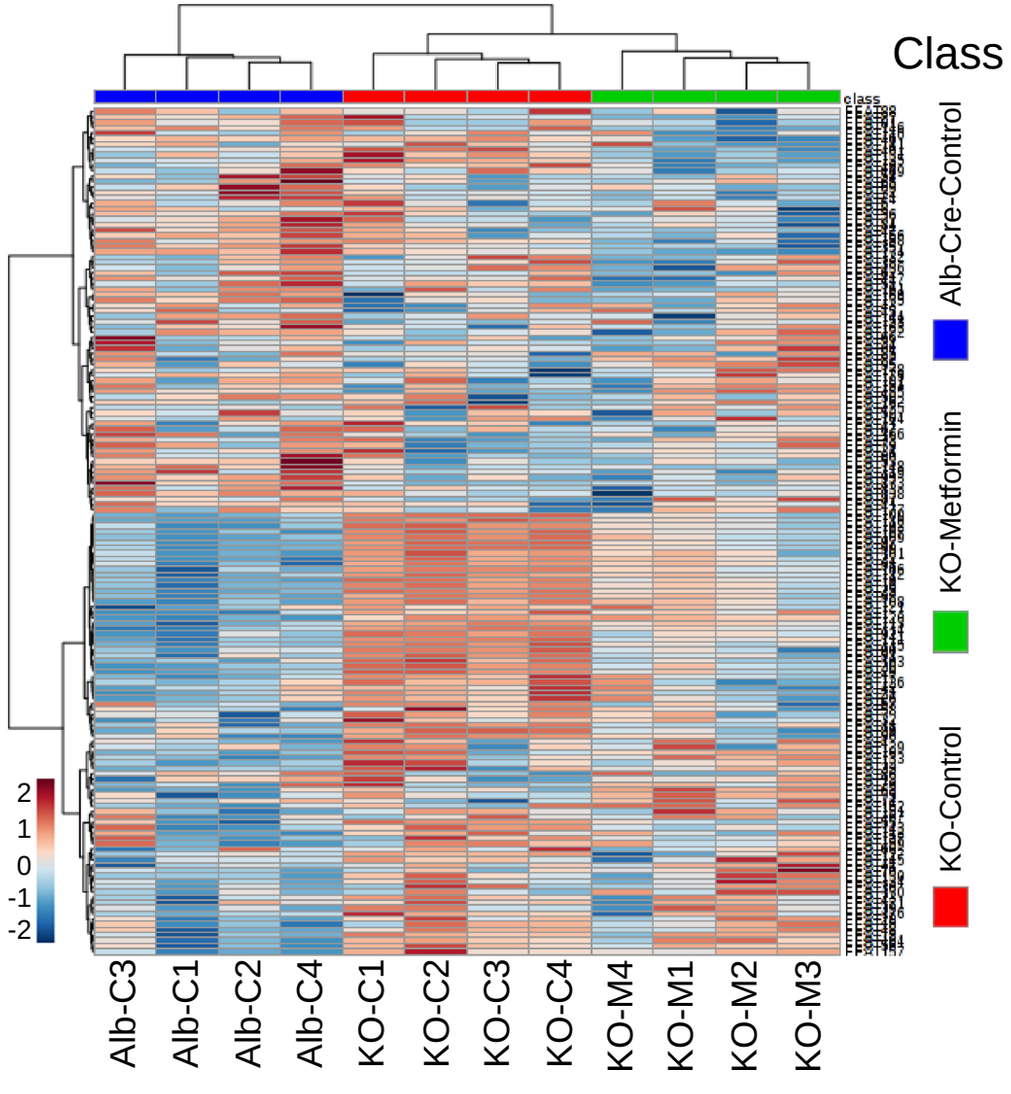
Class
Alb-Cre-Control
KO-Metformin
KO-Control
2
1
0
-1
-2
Alb-C3
Alb-C1
Alb-C2
Alb-C4
KO-C1
KO-C2
KO-C3
KO-C4
KO-M4
KO-M1
KO-M2
KO-M3

Figure S7 (Related to Figure 7): Effect of metformin on mitochondrial Ca^{2+} uptake and Liver lipidomic alterations in $MCU^{\Delta hep}$ mice.

(A) Metformin treatment did not alter $_{m}Ca^{2+}$ uptake in hepatocytes. Hepatocytes isolated from control and metformin administered $MCU^{fl/fl}$ and $MCU^{\Delta hep}$ mice were isolated, permeabilized with digitonin (40 μg/mL) in intracellular like media containing thapsigargin (2 μM), and bathed in the Ca^{2+} indicator Fura2FF (1 μM). After reaching steady state, a bolus of extramitochondrial Ca^{2+} (10 μM) was added at the indicated time point before adding the mitochondrial uncoupler FCCP (2 μM). Representative traces of $[Ca^{2+}]_{out}$ clearance in permeabilized hepatocytes. n=3. **(B)** Metformin administration does not affect the size of the lipid droplets in MCU-KO hepatocytes. Lipid droplets size were quantified after BODIPY® 493/503 staining. Mean ± SEM. ***$p < 0.001$; ns= not significant; n=15-30 cells. **(C)** A one-way ANOVA was performed on the log transformed extracted features obtained from the untargeted analysis of the lipid extract. Those features identified as being significantly different are represented in red while those features which are not significant are represented in green. n=4 mice per group. **(D)** LCMS features extracted from the LCMS analysis of the lipids were subjected to cluster analysis as described in materials and methods. The data reveal a clear separation in the lipidome between control (Alb-Cre-Control), $MCU^{\Delta hep}$ (KO-Control) and metformin treated $MCU^{\Delta hep}$ mice (KO-Metformin). n=4 mice per group.